J. Fluid Mech. (1993), *vol.* 248, *pp.* 477–491

Boundary mixing in stratified reservoirs

By J. IMBERGER AND G. N. IVEY
Centre for Water Research, University of Western Australia, Nedlands 6009, Australia

(Received 14 August 1991 and in revised form 10 October 1992)

We consider the steady flow driven by turbulent mixing in a benthic boundary layer along a sloping boundary in the general case of a non-uniform background density gradient. The velocity and density fields are decomposed into barotropic and baroclinic components, and a solution is obtained by taking an expansion in the small parameter A, the aspect ratio of the boundary layer defined as the thickness divided by the alongslope length. The flow in the boundary layer is governed by a balance between alongslope baroclinic and barotropic density fluxes. A number of flow regimes can exist, and we show that in the regimes relevant to lakes and reservoirs, the barotropic flow is divergent and drives an exchange flow between the boundary layer and the interior. This leads to changes in the interior density gradient which are significant when compared to field observations.

1. Introduction

An important aspect of parameterizing the basin-scale mixing in density-stratified water bodies such as lakes and oceans is to quantify the effects of the energetic turbulent mixing occurring near the sloping bottom boundaries. Munk (1966) was the first to suggest that much of the apparent vertical mixing occurring in the deep ocean basins may be the result of mixing occurring on the sloping bottoms followed by some adjustment process whereby mixed fluid is conveyed into the interior, ultimately resulting in apparent vertical mixing in the interior. This suggestion has subsequently been investigated in field observations (Armi 1978; Gregg & Sanford 1980; Thorpe 1987; Imberger 1989; Ledwell & Watson 1991), in laboratory experiments (Ivey & Corcos 1982; Phillips, Shyu & Salmun 1986; Ivey 1987; Ivey & Nokes 1989) and analytical and numerical studies (e.g. Eriksen 1985; Garrett 1990; Woods 1991; Salmun, Killworth & Blundell 1991).

Many studies have investigated particular mechanisms likely to be responsible for driving mixing at the boundaries of stratified fluids. The candidates are either mean flows over the hydraulically rough bottom or, more likely, mixing driven by the breaking of internal waves on or near the sloping bottom boundaries (e.g. Eriksen 1985; Gilbert & Garrett 1989; Ivey & Nokes 1989). From the point of view of overall mixing, the consequences of any mixing at the boundaries will be the same: the generation of a density anomaly between the turbulent boundary region and the quiescent interior which will result in an adjustment process.

The initial laboratory experiments (Ivey & Corcos 1982; Thorpe 1982) used grid stirring to simulate the boundary mixing in containers with vertical sidewalls. Stratification confined the turbulence to the boundary regions, and because of either the finite depth of the laboratory tank or of variations in the strength of the buoyancy frequency N with depth, as in the case of a two-layer stratification for example, the resulting along boundary turbulent buoyancy flux was divergent. This, in turn, created a density anomaly between the fluid in the turbulent boundary layer

and the quiescent interior, resulting in a horizontal outflow. In the confined geometry of the laboratory tank, an overall circulation was set up with a slow vertical advection in the interior weakening the interior density gradient, a temporal evolution which Woods (1991) has shown can be described by a similarity solution for the case with steady mixing at the boundaries.

These initial laboratory studies have been extended to include the effects of both rotation and sloping sides. Ivey (1987) incorporated the effects of rotation by using a vertically oscillating grid to drive mixing in the centre of a cylindrical tank filled with a stratified fluid and mounted on a rotating turntable. While the dynamics of mixing in the turbulent boundary layer which formed near the oscillating grid were unaffected by rotation, the resulting horizontal outflow into the quiescent interior was strongly influenced by the rotation. Rather than a geostrophic balance with azimuthal currents developing around the boundary, the outflow was unstable to rotational instabilities of transitional character between the barotropic and baroclinic regimes. The instabilities rapidly grew and subsequently broke down to form an eddy field which efficiently stirred fluid pumped out of the boundary layer over the horizontal width of the tank. The combined effects of the continual mixing at the boundary and the eddy stirring in the interior again lead to a weakening of the interior density gradient.

While these experiments considered only vertical sides, Phillips (1970) and Wunsch (1970) had earlier considered the effects of a sloping bottom in a container with a uniform stratification and a uniform diffusivity throughout the flow field. In order to satisfy the no-flux condition at the boundary, the isopycnals must bend near the boundaries so that the gradient normal to the wall vanishes, and the resulting buoyancy forces drive a net flow up the slope. The magnitude of this flow can be evaluated directly by consideration of the flux balances in the control volume shown in figure 1. For steady state

$$\text{convective flux in} - \text{convective flux out} = \text{diffusive flux out},$$

$$q\rho_{\text{in}} - q\rho_{\text{out}} = q\frac{\partial \rho}{\partial x}L = \epsilon\frac{\partial \rho}{\partial Z}L\cos\theta,$$

$$q\frac{\partial \rho}{\partial Z}\sin\theta = \epsilon\frac{\partial \rho}{\partial Z}\cos\theta,$$

$$q = \epsilon\cot\theta.$$

Thus the strength of the flow q up the boundary is directly proportional to the interior diffusivity ϵ. In lakes this interior diffusivity is essentially molecular (e.g. Imberger 1989) and thus the flow q up the slope is very weak. Thorpe (1987) extended the solution to incorporate the effects of rotation and, while rotation does induce an alongslope flow outside the boundary layer, the upslope flow is still given by the above equations and is thus vanishingly small if the interior diffusivity is molecular or near-molecular.

The laboratory experiment of Phillips *et al.* (1986) and Salmun & Phillips (1992) used an oscillating grid to create a turbulent region along the sloping bottom boundary. As in the case of the vertical wall experiments, the stratification confined the turbulent region to the vicinity of the bottom slope and the authors suggested that the alongslope flow in this region became bi-directional – upslope close to the boundary and downslope outside – although the net volume flux associated with this secondary or baroclinic flow was zero. The shear in this baroclinic flow normal to the

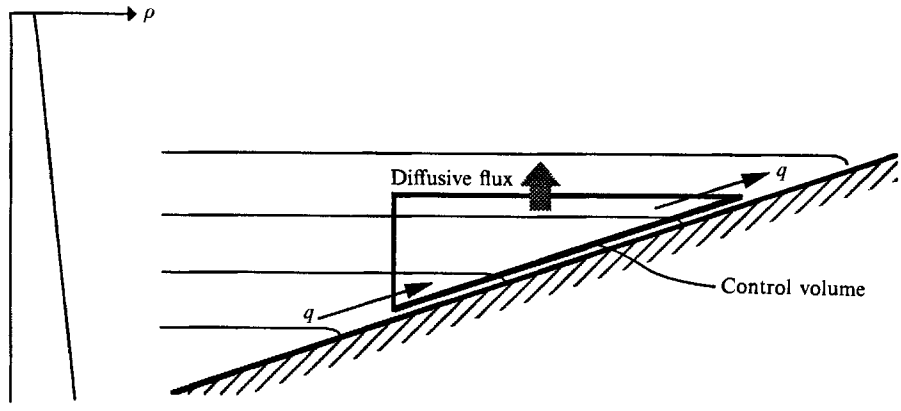

FIGURE 1. Schematic of diffusively driven transport q along a sloping boundary.

boundary does, however, lead to a shear flow dispersive transport along the slope. In the case where the background stratification was non-uniform, as when a pycnocline was present, this alongslope dispersive transport created density differences between the boundary regions and the interior and a mean or barotropic flow resulted. This barotropic flow was convergent at the pycnocline and lead to an intruding flow from the boundary layer into the interior. No quantitative observations were made of either this baroclinic flow or of the convergent barotropic flow to support these ideas, and observations were confined to measurements of the temporal evolution of the interior stratification.

Garrett (1990, 1991) examined the steady baroclinic or secondary flow for the case of uniform stratification and argued that the total alongslope buoyancy flux in this unidirectional flow situation consisted of both a shear-driven dispersive component, as described by Phillips *et al.* (1986), and a direct diffusive component. He concluded that the total flux could in fact be less than the value given by the turbulent diffusive flux acting alone, where the degree of reduction depends on the relative thickness of the buoyancy boundary-layer scale δ and the thickness of the region h over which the eddy coefficients decreased from their value on the boundary to the assumed zero value in the interior. If h/δ was greater than 1, then the total flux approached that given by the alongslope turbulent diffusive term acting alone. In all cases considered, there was either no barotropic flow or the barotropic flow was constant along the boundary (e.g. Young & Jones 1991) and thus there was no exchange flow between the boundary layer and the quiescent interior.

Salmun *et al.* (1991) extended these one-dimensional models by considering the steady two-dimensional flow along a sloping bottom with a turbulent bottom boundary layer. Ignoring the effects of rotation, they considered the nature of the flow when the background linear stratification was perturbed by some arbitrary, but assumed small, amount about a uniform value. At zeroth order, their problem is essentially a balance between buoyancy and viscous forces, as considered by Phillips (1970), Thorpe (1987) and Garrett (1990), with the property that if the stratification is uniform there is no exchange flow between the boundary layer and the interior. At the next order, they argued that the problem becomes a three way balance between inertia, buoyancy and viscosity and a series of numerical solutions were presented for varying boundary-layer thicknesses, scale height of the stratification and turbulent diffusivities in the boundary layer. The solutions yielded insight into the character of the two-dimensional flow, but the relative magnitudes of the baroclinic and

barotropic velocities, the basic force balances that prevail, and the range of validity of the solutions were not clear.

All these studies considered steady flows and the unsteady aspects of boundary mixing have only recently received attention (e.g. Garrett 1991). In the rotating case, in addition to the effect on interior stratification, boundary mixing influences the interior velocity field and MacCready & Rhines (1991) showed that once Thorpe's (1987) steady solution for the alongslope flow was established, the velocity outside the boundary layer slowly diffused into the interior. In terms of the boundary-layer properties themselves, the field observations of Thorpe, Hall & White (1990) indicated that temporal variability of the mixing was likely, although such considerations are beyond the scope of the present study.

Motivated by observations from a recent field experiment in Lake Argyle, in §2 below we extend this earlier work and describe a fully analytical two-dimensional model to describe the flow on a sloping bottom boundary in a stratified fluid. We consider only steady flows and ignore the effects of rotation in such relatively small water bodies. The bottom slope is small and uniform, as is the strength of the turbulence, although the stratification is non-uniform. The model differs from that described by Salmun *et al.* (1991) in two fundamental ways. Firstly, recognizing that the flow field consists of two distinct components, at the outset we decompose the velocity and density fields into two components: a barotropic component and a baroclinic component, with the property that the integral over the depth of the turbulent boundary-layer thickness h of the baroclinic components vanishes. Secondly, rather than an arbitrary perturbation parameter, we use the naturally occurring small parameter A as the perturbation parameter, where A is defined as the ratio of the turbulent boundary-layer thickness h, measured perpendicular to the slope, divided by the lengthscale L, the alongslope scale over which the background stratification changes.

As we show below, a formal expansion of the flow variables in the parameter A enables an analytic solution to the flow to be found. This approach has the advantage of defining a number of possible flow regimes, one of which is the regime considered by Salmun *et al.* (1991) in which inertia is important. We show, however, that at least for smaller bodies inertia terms are small compared to the viscous and buoyancy terms. In this regime a divergent barotropic flow can be set up in the boundary layer which leads to a net discharge or exchange flow with the interior, hence forcing changes in the interior density stratification.

2. Boundary flux

Consider the flow induced by a longitudinal density gradient formed by boundary mixing along a sloping wall as shown in figure 2. The momentum and species equations under the Boussinesq approximation for steady flow in the benthic boundary layer are

$$\rho_0\left\{u\frac{\partial u}{\partial x}+w\frac{\partial u}{\partial z}\right\}=-\frac{\partial P}{\partial x}-\rho g\sin\theta+\rho_0\epsilon\left\{\frac{\partial^2 u}{\partial z^2}+\frac{\partial^2 u}{\partial x^2}\right\}, \tag{1}$$

$$\rho_0\left\{u\frac{\partial w}{\partial x}+w\frac{\partial w}{\partial z}\right\}=-\frac{\partial P}{\partial z}-\rho g\cos\theta+\rho_0\epsilon\left\{\frac{\partial^2 w}{\partial z^2}+\frac{\partial^2 w}{\partial x^2}\right\}, \tag{2}$$

$$u\frac{\partial \rho}{\partial x}+w\frac{\partial \rho}{\partial z}=\epsilon\left\{\frac{\partial^2 \rho}{\partial x^2}+\frac{\partial^2 \rho}{\partial z^2}\right\}, \tag{3}$$

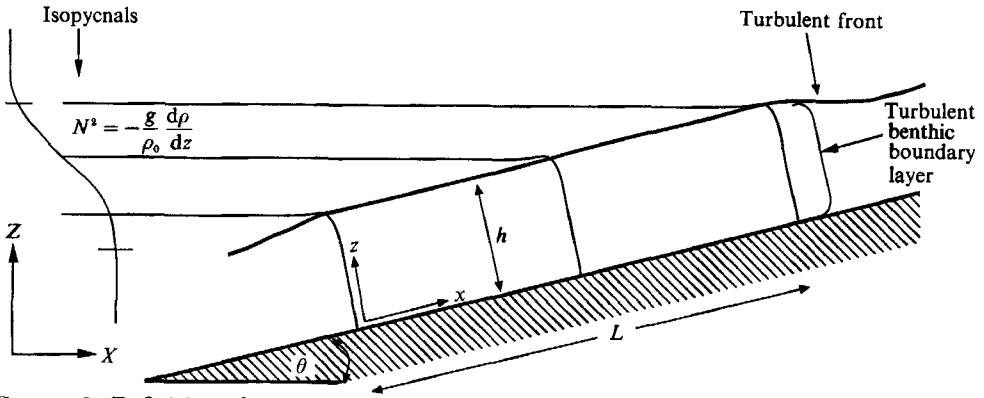

FIGURE 2. Definition of coordinates and parameters for a model of the flow along the sloping turbulent boundary layer.

where u and w are the mean velocities in the x- and z-directions, P is the mean pressure, ρ_0 is the average mean density, ρ is the mean density anomaly above ρ_0 and ϵ is the turbulent exchange coefficient, assumed the same for mass and momentum.

Now eliminating the pressure between (1) and (2) yields the mean vorticity equation:

$$\rho_0\frac{\partial}{\partial z}\left\{u\frac{\partial u}{\partial x}+w\frac{\partial u}{\partial z}\right\}-\rho_0\frac{\partial}{\partial x}\left\{u\frac{\partial w}{\partial x}+w\frac{\partial w}{\partial z}\right\}$$

$$=-g\sin\theta\frac{\partial\rho}{\partial z}+g\cos\theta\frac{\partial\rho}{\partial x}+\rho_0\epsilon\frac{\partial^3 u}{\partial z^3}+\rho_0\epsilon\frac{\partial^3 u}{\partial z\,\partial x^2}-\rho_0\epsilon\frac{\partial^3 w}{\partial x^3}-\rho_0\epsilon\frac{\partial^3 w}{\partial x\,\partial z^2}. \quad (4)$$

The mean velocity field is assumed to be made up of two distinct flows: components $\tilde{u}$ and $\tilde{w}$ describing the discharge flow, and baroclinic components u' and w' driven by the longitudinal density distribution. Hence let

$$u(x,z)=\tilde{u}(x,z)+u'(x,z); \quad w(x,z)=\tilde{w}(x,z)+w'(x,z) \quad (5)$$

with the property

$$\int_0^h u(x,z)\,dz = q = \int_0^h \tilde{u}(x,z)\,dz. \quad (6)$$

Thus from conservation of mass

$$\frac{dq}{dx}=-\tilde{w}|_h \quad \text{and} \quad w'|_h=0. \quad (7)$$

Similarly, the density variation may be divided into two components: the longitudinal variation $\Lambda(x)$, and the density perturbation $\rho'(x,z)$ induced by the flow, so that

$$\rho(x,z)=\Lambda(x)+\rho'(x,z). \quad (8)$$

Consider now the scales associated with these variables.

$$\tilde{u}\sim q/h \quad (9)$$

and

$$\Lambda\sim\Delta\rho, \quad (10)$$

where $\Delta\rho$ is the density difference between the two ends of the flow domain.

The flow is confined within the turbulent boundary layer and if we assume that the aspect ratio

$$h/L=A\ll 1 \quad (11)$$

then it is reasonable to assume that to first order

$$g\cos\theta\,\partial\Lambda/\partial x \sim \rho_0\,\epsilon\,\partial^3 u'/\partial z^3, \tag{12}$$

$$u'\,\partial\Lambda/\partial x \sim \epsilon\,\partial^2\rho'/\partial z^2, \tag{13}$$

and at second order

$$\tilde{u}\,\partial\Lambda/\partial x \sim (\partial/\partial x)\,(u'\rho'). \tag{14}$$

Equation (12) states that the baroclinic velocity field is forced by the longitudinal gradient, the resistance to the forcing being internal friction. Equation (13) is the classical Taylor (1954) assumption underlying longitudinal dispersion and (14) assumes that the barotropic volume flux keeps the flow in steady state.

If we let

$$u' \sim U, \tag{15}$$

$$\tilde{u} \sim q/h, \tag{16}$$

$$\rho' \sim \delta\rho, \tag{17}$$

and

$$\Lambda \sim \Delta\rho, \tag{18}$$

then (12)–(14) imply

$$U \sim Gr\,\epsilon/L, \tag{19}$$

$$\delta\rho/\Delta\rho \sim Gr\,A^2 \tag{20}$$

and

$$q \sim Gr^2 A^3 \epsilon, \tag{21}$$

where the Grashof number

$$Gr = \frac{g\Delta\rho}{\rho}\frac{h^3}{\epsilon^2}\cos\theta. \tag{22}$$

Equations (3) and (4) can be non-dimensionalized by introducing the new variables

$$u' = u'/U, \quad w' = A u', \tag{23}$$

$$\tilde{u} = \tilde{u}h/q, \quad \tilde{w} = A\tilde{u}, \tag{24}$$

$$\Lambda = \Lambda/\Delta\rho, \tag{25}$$

$$\rho = \rho'/\delta\rho, \tag{26}$$

$$x = x/L, \tag{27}$$

$$z = z/h, \tag{28}$$

where we have not introduced separate variables to differentiate between physical and non-dimensional variables. The non-dimensional forms for (3) and (4) become, after substituting (5), (8), and (23)–(28):

$$\begin{aligned}
&Gr^3A^6\frac{\partial}{\partial z}\left(\tilde{u}\frac{\partial\tilde{u}}{\partial x}\right)+Gr^2A^4\frac{\partial}{\partial z}\left(\tilde{u}\frac{\partial u'}{\partial x}+u'\frac{\partial\tilde{u}}{\partial x}\right)+GrA^2\frac{\partial}{\partial z}\left(u'\frac{\partial u'}{\partial x}\right)\\
&\quad+Gr^3A^6\frac{\partial}{\partial x}\left(\tilde{w}\frac{\partial\tilde{u}}{\partial x}\right)+Gr^2A^4\frac{\partial}{\partial x}\left(\tilde{w}\frac{\partial u'}{\partial x}+w'\frac{\partial\tilde{u}}{\partial x}\right)+GrA^2\frac{\partial}{\partial x}\left(w'\frac{\partial u'}{\partial x}\right)\\
&\quad-Gr^3A^8\frac{\partial}{\partial x}\left(\tilde{u}\frac{\partial\tilde{w}}{\partial x}\right)-Gr^2A^6\frac{\partial}{\partial x}\left(\tilde{u}\frac{\partial w'}{\partial x}+u'\frac{\partial\tilde{w}}{\partial x}\right)-GrA^4\frac{\partial}{\partial x}\left(u'\frac{\partial w'}{\partial x}\right)\\
&\quad-Gr^3A^8\frac{\partial}{\partial x}\left(\tilde{w}\frac{\partial\tilde{w}}{\partial x}\right)-Gr^2A^6\frac{\partial}{\partial x}\left(\tilde{w}\frac{\partial w'}{\partial x}+w'\frac{\partial\tilde{w}}{\partial x}\right)-GrA^4\frac{\partial}{\partial x}\left(w'\frac{\partial w'}{\partial x}\right)\\
&=-GrA\tan\theta\frac{\partial\rho'}{\partial z}+GrA^2\frac{\partial\rho'}{\partial z}+\frac{\mathrm{d}\Lambda}{\mathrm{d}x}\\
&\quad+GrA^4\frac{\partial^3\tilde{u}}{\partial x^2\,\partial z}+A^2\frac{\partial^3u'}{\partial x^2\,\partial z}+GrA^2\frac{\partial^3\tilde{u}}{\partial z^3}+\frac{\partial^3u'}{\partial z^3}\\
&\quad-GrA^6\frac{\partial^3\tilde{w}}{\partial x^3}-A^4\frac{\partial^3w'}{\partial x^2}-GrA^4\frac{\partial^3\tilde{w}}{\partial x\,\partial z^2}-A^2\frac{\partial^3w'}{\partial x\,\partial z^2}
\end{aligned} \tag{29}$$

and

$$Gr^2A^2\tilde{u}\frac{\mathrm{d}\Lambda}{\mathrm{d}x}+Gr\,u'\frac{\mathrm{d}\Lambda}{\mathrm{d}x}+Gr^3A^4\left(\tilde{u}\frac{\partial\rho'}{\partial x}+\tilde{w}\frac{\partial\rho'}{\partial x}\right)$$
$$+Gr^2A^2\left(u'\frac{\partial\rho'}{\partial x}+w'\frac{\partial\rho'}{\partial z}\right)=\frac{\mathrm{d}^2\Lambda}{\mathrm{d}x^2}+GrA^2\frac{\partial^2\rho'}{\partial x^2}+Gr\frac{\partial^2\rho'}{\partial z^2}. \quad (30)$$

As discussed in §3 below, for lakes A is about 10^{-3} and a perturbation solution in small A is thus likely to be successful. However, before this can be done it is necessary to order Gr relative to the magnitude of A, so that the two-parameter equations reduce to a one-parameter system of equations.

Cormack, Leal & Imberger (1974) assumed $Gr = O(1)$ as $A \to 0$. Taking a regular expansion in the small parameter A in (29) and (30) yields to first order

$$Gr\,u_0'\frac{\mathrm{d}\Lambda_0}{\mathrm{d}x}=\frac{\mathrm{d}^2\Lambda_0}{\mathrm{d}x^2}+Gr\frac{\partial^2\rho_0'}{\partial z^2} \quad (31)$$

and

$$\frac{\partial^3u_0'}{\partial z^3}+\frac{\mathrm{d}\Lambda_0}{\mathrm{d}x}=0. \quad (32)$$

As discussed in §1, the density flux in the interior is vanishingly small, thus integrating (31) with respect to z between 0 and 1, and setting $\partial\rho_0'/\partial z = 0$ at $z = 0$ and $z = 1$ yields, to a good approximation, the simple result

$$\mathrm{d}^2\Lambda_0/\mathrm{d}x^2=0. \quad (33)$$

Similarly

$$\mathrm{d}^2\Lambda_1/\mathrm{d}x^2=0. \quad (34)$$

In other words the density gradient is linear with x, the flow is parallel and the discharge flow defined in (6) is zero.

Bejan & Imberger (1979) investigated the case where $Gr = O(A^{-1})$ but did not require (14). Again expanding the variables in powers of A yields at first order

$$u_0'\,\mathrm{d}\Lambda_0/\mathrm{d}x=\partial^2\rho_0'/\partial z^2, \quad (35)$$

which requires zero mass flux at $z = 0$ and 1. The second-order equation becomes

$$\tilde{u}_0\frac{\mathrm{d}\Lambda_0}{\mathrm{d}x}+u_1'\frac{\mathrm{d}\Lambda_0}{\mathrm{d}x}+u_0'\frac{\mathrm{d}\Lambda_1}{\mathrm{d}x}+u_0'\frac{\partial\rho_0'}{\partial x}+w_0'\frac{\partial\rho_0'}{\partial x}=\frac{\mathrm{d}^2\Lambda_0}{\mathrm{d}x^2}+\frac{\partial^2\rho_1'}{\partial z^2}. \quad (36)$$

On integration with respect to z between 0 and 1 (36) reduces to

$$q\frac{\mathrm{d}\Lambda_0}{\mathrm{d}x}+\frac{\mathrm{d}}{\mathrm{d}x}\int_0^1(u_0'\rho_0')\,\mathrm{d}z=\frac{\mathrm{d}^2\Lambda_0}{\mathrm{d}x^2}, \quad (37)$$

where we have used the conditions $w_0'\rho_0'|_0^1 = 0$ and the non-dimensional discharge $q = \int_0^1 \tilde{u}_0\,\mathrm{d}z$.

Given that u_0' follows directly from the first-order balance in (32) and ρ_0' from (35), this yields an equation for Λ_0. Equation (37) is a generalization of that derived by Bejan & Imberger (1979) who did not include the baroclinic flux term, required by the inclusion of (14) in the present derivation. Equation (37) clearly shows that a perturbation scheme based on the balance in (35) will always retain the longitudinal diffusion term and the net discharge q is balanced by the diffusive flux and the Taylor dispersion.

By assuming $Gr = O(A^{-2})$ equation (29) yields a balance at leading order between inertia, buoyancy and internal friction. Under such a balance the layer thickness is limited by the advective acceleration terms and the equations are fully nonlinear. However, typical values in lakes discussed in §3 below indicate that the inertia terms are in fact small compared to the buoyancy terms.

The magnitudes of Gr and A thus suggest the ordering

$$Gr = A^{-\frac{3}{2}}, \tag{38}$$

which yields a discharge so that the advective flux balances the diffusive flux. This yields in the limit $A \to 0$

$$Gr^2 A^2 = A^{-1} \to \infty \tag{39}$$

and

$$Gr A^2 = A^{\frac{1}{2}} \to 0 \tag{40}$$

as required by the nature of the problem for A small. Given (38), (29) and (30) reduce to

$$\begin{aligned}
&A^{\frac{3}{2}}\frac{\partial}{\partial z}\left(\tilde{u}\frac{\partial \tilde{u}}{\partial x}\right)+A\frac{\partial}{\partial z}\left(\tilde{u}\frac{\partial u'}{\partial x}+u'\frac{\partial \tilde{u}}{\partial x}\right)+A^{\frac{1}{2}}\frac{\partial}{\partial z}\left(u'\frac{\partial u'}{\partial x}\right)\\
&\quad+A^{\frac{3}{2}}\frac{\partial}{\partial z}\left(\tilde{w}\frac{\partial \tilde{u}}{\partial z}\right)+A\frac{\partial}{\partial z}\left(\tilde{w}\frac{\partial u'}{\partial x}+w'\frac{\partial \tilde{u}}{\partial x}\right)+A^{\frac{1}{2}}\frac{\partial}{\partial z}\left(w'\frac{\partial w'}{\partial z}\right)\\
&\quad-A^{\frac{7}{2}}\frac{\partial}{\partial x}\left(\tilde{u}\frac{\partial \tilde{w}}{\partial x}\right)-A^{3}\frac{\partial}{\partial x}\left(\tilde{u}\frac{\partial w'}{\partial x}+u'\frac{\partial \tilde{w}}{\partial x}\right)-A^{\frac{5}{2}}\frac{\partial}{\partial z}\left(u'\frac{\partial w'}{\partial x}\right)\\
&\quad-A^{\frac{7}{2}}\frac{\partial}{\partial x}\left(\tilde{w}\frac{\partial \tilde{w}}{\partial z}\right)-A^{3}\frac{\partial}{\partial x}\left(\tilde{w}\frac{\partial w'}{\partial z}+w'\frac{\partial \tilde{w}}{\partial z}\right)-A^{\frac{5}{2}}\frac{\partial}{\partial z}\left(w'\frac{\partial w'}{\partial z}\right)\\
&=-A^{-\frac{1}{2}}\tan\theta\frac{\partial \rho'}{\partial z}+A^{\frac{1}{2}}\frac{\partial \rho'}{\partial x}+\frac{\mathrm{d}\Lambda}{\mathrm{d}x}+A^{\frac{5}{2}}\frac{\partial^3 \tilde{u}}{\partial x^2\,\partial z}+A^{2}\frac{\partial^3 u'}{\partial x^2\,\partial z}+A^{\frac{1}{2}}\frac{\partial^3 \tilde{u}}{\partial z^3}+\frac{\partial^3 u'}{\partial z^3}\\
&\quad-A^{\frac{9}{2}}\frac{\partial^3 \tilde{w}}{\partial x^3}-A^{4}\frac{\partial^3 w'}{\partial x^3}-A^{\frac{5}{2}}\frac{\partial^3 \tilde{w}}{\partial x\,\partial z^2}-A^{2}\frac{\partial^3 w'}{\partial x\,\partial z^2}
\end{aligned} \tag{41}$$

and

$$A^{\frac{1}{2}}\tilde{u}\frac{\mathrm{d}\Lambda}{\mathrm{d}x}+u'\frac{\mathrm{d}\Lambda}{\mathrm{d}x}+A\left(\tilde{u}\frac{\partial \rho'}{\partial x}+\tilde{w}\frac{\partial \rho'}{\partial z}\right)+A^{\frac{1}{2}}\left(u'\frac{\partial \rho'}{\partial x}+w'\frac{\partial \rho'}{\partial z}\right)=A^{\frac{3}{2}}\frac{\mathrm{d}^2\Lambda}{\mathrm{d}x^2}+A^{2}\frac{\partial^2 \rho'}{\partial x^2}+\frac{\partial^2 \rho'}{\partial z^2}. \tag{42}$$

Consider a solution where the variables $\tilde{u}$, u', $\tilde{w}$, w', Λ and ρ' can be expanded in the form

$$\phi = \phi_0 + A^{\frac{1}{2}}\phi_1 + A\phi_2 + \ldots. \tag{43}$$

If we define a new parameter α by

$$A^{-\frac{1}{2}}\tan\theta = \alpha \tag{44}$$

then substituting expansions of the form of (43) into (41) and (42) leads to the following sets of equations at first and second order:

A^0:

$$\frac{\partial^3 u_0'}{\partial z^3} = -\frac{\mathrm{d}\Lambda_0}{\mathrm{d}x}+\alpha\frac{\partial \rho'}{\partial z}, \tag{45}$$

$$u_0'\frac{\mathrm{d}\Lambda_0}{\mathrm{d}x} = \frac{\partial^2 \rho_0'}{\partial z^2}; \tag{46}$$

$A^{\frac{1}{2}}$:
$$\frac{\partial}{\partial z}\left(u_0'\frac{\partial u_0'}{\partial x}\right)+\frac{\partial}{\partial z}\left(w_0'\frac{\partial u_0'}{\partial z}\right)=\frac{\partial^3\tilde{u}_0}{\partial z^3}+\frac{\partial^3 u_1'}{\partial z^3}+\frac{\mathrm{d}\Lambda_1}{\mathrm{d}x}+\frac{\partial\rho_0'}{\partial x}-\alpha\frac{\partial\rho_1'}{\partial z}, \tag{47}$$

$$\tilde{u}_0\frac{\mathrm{d}\Lambda_0}{\mathrm{d}x}+u_0'\frac{\mathrm{d}\Lambda_1}{\mathrm{d}x}+u_1'\frac{\mathrm{d}\Lambda_0}{\mathrm{d}x}+\frac{\partial}{\partial x}(u_0'\rho_0')+\frac{\partial}{\partial z}(w_0'\rho_0')=\frac{\partial^2\rho_1'}{\partial z^2}. \tag{48}$$

The parameter α is determined by the geometry and if α is of order one, then the balance in (12) becomes

$$g\sin\theta\frac{\partial\rho'}{\partial z}-g\cos\theta\frac{\partial\Lambda}{\partial x}\sim\rho_0\frac{\partial^3 u'}{\partial z^3}. \tag{49}$$

At order A^0, the solution of (45) and (46) is (cf. Phillips 1970)

$$u_0'(x,z)=\frac{1}{2}\left(\frac{\mathrm{d}\Lambda_0}{\mathrm{d}x}\right)\frac{\beta}{\sinh\beta+\sin\beta}\left\{\frac{\sinh\beta(z-1)\sin\beta z-\sinh\beta z\sin\beta(z-1)}{\beta^4}\right\}, \tag{50}$$

$$\rho_0'(x,z)=-\frac{1}{4}\left(\frac{\mathrm{d}\Lambda_0}{\mathrm{d}x}\right)^2\frac{\beta}{\sinh\beta+\sin\beta}$$
$$\times\left\{\frac{\cosh\beta(z-1)\cos\beta z-\cosh\beta z\cos\beta(z-1)}{\beta^6}+\frac{\beta(\sinh\beta+\sin\beta)\,(z-\frac{1}{2})}{\beta^6}\right\}, \tag{51}$$

where
$$\beta^4=-\tfrac{1}{4}\alpha\,\mathrm{d}\Lambda_0/\mathrm{d}x. \tag{52}$$

In the limit $\alpha\to 0$, the solutions of (45) and (46) are

$$u_0'=-(\mathrm{d}\Lambda_0/\mathrm{d}x)\,(\tfrac{1}{6}z^3-\tfrac{1}{4}z^2+\tfrac{1}{12}z), \tag{53}$$

$$\rho_0'=-(\mathrm{d}\Lambda_0/\mathrm{d}x)^2\,(\tfrac{1}{120}z^5-\tfrac{1}{48}z^4+\tfrac{1}{72}z^3-\tfrac{1}{1440}), \tag{54}$$

where we have assumed that

$$u_0'=0,\quad z=0,1, \tag{55}$$

$$\partial\rho_0'/\partial z=0,\quad z=0,1. \tag{56}$$

While the boundary condition (55) implies that there will be a stress jump at the interface between the turbulent and non-turbulent fluid at $z=1$, it is realistic in confining the baroclinic velocity signature to the turbulent region. More importantly, the use of a stress-free boundary condition leads to only slight modification of the coefficient γ calculated below.

Consider now the species equation at second order; then integrating (48) with respect to z between 0 and 1 yields

$$q\left(\frac{\mathrm{d}\Lambda_0}{\mathrm{d}x}\right)+\frac{\mathrm{d}}{\mathrm{d}x}\int_0^1(u_0'\rho_0')\,\mathrm{d}z+w_0'\rho_0'\Big|_0^1=\frac{\partial\rho_1'}{\partial z}\Big|_0^1. \tag{57}$$

Using (56), noting that $w_0'\rho_0'|_0^1=0$ and substituting (50) and (51) leads to the expression

$$q\frac{\mathrm{d}\Lambda_0}{\mathrm{d}x}+3\left(\frac{\mathrm{d}\Lambda_0}{\mathrm{d}x}\right)^2\frac{\mathrm{d}^2\Lambda_0}{\mathrm{d}x^2}\gamma=0, \tag{58}$$

where

$$\gamma=-\int_0^1\frac{1}{8\beta^8(\sinh\beta+\sin\beta)^2}\{\sinh\beta(z-1)\sin\beta z-\sinh\beta z\sin\beta(z-1)\}$$
$$\times\{\cosh\beta(z-1)\cos\beta z-\cosh\beta z\cos\beta(z-1)+\beta(\sinh\beta+\sin\beta)\,(z-\tfrac{1}{2})\}\,\mathrm{d}z. \tag{59}$$

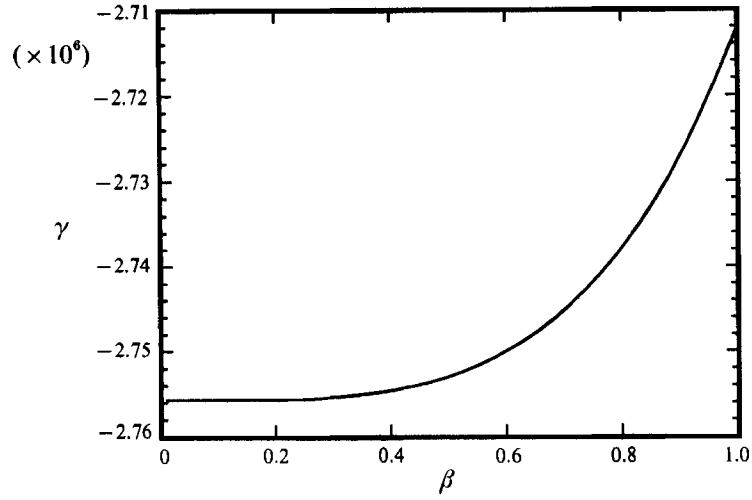

FIGURE 3. The dependence of parameter γ on β as defined in equations (59) and (52), respectively.

From the field date summarized in table 1 below, it is clear that $\alpha < 1$, and taking the stratification of the form in (60) below, then $\beta < 1$ also. In figure 3 we show the results of the integrations in (59) for this range. It is clear that γ is only a weak function of β and the magnitude of γ is greatest, and hence the discharge q in (58) is greatest, when $\beta \to 0$ and $\gamma = -2.7557 \times 10^{-6}$.

Equation (58) yields an expression for q given any distribution for A_0. This is quite different to the case where $Gr = O(1)$, $O(A^{-1})$ and $O(A^{-2})$ where the force balance determines the distribution of A_0. When $Gr = O(1)$, there is no discharge; when $Gr = O(A^{-1})$, q is fixed by longitudinal diffusion; when $Gr = O(A^{-\frac{3}{2}})$, q is fixed by the convective flux; and when $Gr = O(A^{-2})$, q is fixed by the advective flux (nonlinear).

In the present case with $Gr = O(A^{-\frac{3}{2}})$, we can assume without loss of generality that

$$A_i = 0 \quad \text{for all} \quad i \geqslant 1.$$

3. Discussion

Consider the case where the stratification can be described by a simple sinusoidal stratification of the form

$$A(x) = \tfrac{1}{2}\cos \pi x + \tfrac{1}{2}, \quad 0 < x < 1. \tag{60}$$

Then from (58), the discharge is

$$q(x) = -\tfrac{3}{8}\pi^3 \gamma \sin 2\pi x; \tag{61}$$

the barotropic flow thus converges towards $x = 0.5$ and the flow detrains over the central portion of the slope where $0.25 < x < 0.75$. The velocity component at the edge of the boundary layer is given by

$$w(z = 1)/\sin\theta = U_{\mathrm{I}}, \tag{62}$$

where U_{I} is the horizontal velocity in the density-stratified interior. In a bounded reservoir or lake, this flow will drive a slow interior circulation, and changes in the interior density gradient will thus occur by slow vertical advection. The magnitude of these changes can be assessed by an advective interior eddy diffusivity defined by

$$w_{\mathrm{I}} \partial\rho/\partial Z = K_{\mathrm{I}} \partial^2\rho/\partial Z^2$$

N (rad s^{-1})	θ (rad)	ϵ (m^2 s^{-1})	h (m)	A	Gr	GrA^2	α
0.001	10^{-3}	10^{-5}	7.2	7.2×10^{-3}	3.7×10^{6}	1.9×10^{2}	1.2×10^{-2}
0.001	10^{-3}	10^{-6}	3.3	3.3×10^{-3}	3.6×10^{7}	3.9×10^{2}	1.7×10^{-2}
0.001	10^{-2}	10^{-5}	3.3	3.3×10^{-3}	3.6×10^{6}	3.9×10^{1}	1.7×10^{-1}
0.01	10^{-3}	10^{-5}	2.6	2.6×10^{-3}	1.8×10^{7}	1.2×10^{2}	2.0×10^{-2}
0.01	10^{-2}	10^{-4}	2.6	2.6×10^{-3}	1.8×10^{6}	1.2×10^{1}	2.0×10^{-1}
0.01	10^{-2}	10^{-5}	1.2	1.2×10^{-3}	1.7×10^{7}	2.4×10^{1}	2.9×10^{-1}
0.01	10^{-2}	10^{-6}	0.55	5.5×10^{-4}	1.8×10^{8}	5.4×10^{1}	4.3×10^{-1}
0.10	10^{-3}	10^{-5}	0.92	9.2×10^{-4}	7.8×10^{7}	6.6×10^{1}	3.3×10^{-2}
0.10	10^{-2}	10^{-4}	0.92	9.2×10^{-4}	7.8×10^{6}	6.6×10^{0}	3.3×10^{-1}
0.10	10^{-2}	10^{-5}	0.43	4.3×10^{-4}	8.2×10^{7}	1.5×10^{1}	4.8×10^{-1}
0.10	10^{-2}	10^{-6}	0.20	2.0×10^{-4}	8.1×10^{8}	3.2×10^{1}	7.1×10^{-1}

TABLE 1. Required boundary-layer thicknesses for $K_1 = 10^{-6}$ m^2 s^{-1} and $l = 10^3$ m $\approx L$.

or
$$K_{\mathrm{I}} = (q/l)\,(\partial\rho/\partial Z)/\partial^2\rho/\partial Z^2, \tag{63}$$

where l is the basin width.

Now from (58), the discharge q in dimensional form is

$$q = -\frac{3\gamma Gr^2 A^3 \epsilon L^3 \sin^3\theta}{(\Delta\rho)^2}\left(\frac{\mathrm{d}A}{\mathrm{d}Z}\right)\left(\frac{\mathrm{d}^2A}{\mathrm{d}Z^2}\right). \tag{64}$$

Note from (64) that if the density gradient were perfectly linear, the discharge q is zero and hence K_{I} would be zero. Substituting into (63) and using the definition of Grashoff number given in (22) yields

$$K_{\mathrm{I}} = -\frac{3\gamma h^9 \cos^2\theta \sin^3\theta}{\epsilon^3 l}\left(\frac{g}{\rho}\frac{\mathrm{d}A}{\mathrm{d}Z}\right)^2. \tag{65}$$

If the stratification is given by a simple sinusoid of the form in (60), and if we take $\gamma = -2.7557\times10^{-6}$, then (65) simplifies to

$$K_{\mathrm{I}} = 2.04\times10^{-5}\left(\frac{N^4h^9\sin^3\theta\cos^2\theta}{\epsilon^3 l}\right)\sin^2\left(\frac{\pi x}{L}\right), \tag{66}$$

where $N^2 = (g/\rho)\,(\Delta\rho/L\sin\theta)$. Thus in this case the interior diffusivity varies from a maximum at $x = \frac{1}{2}L$ and tends to zero as $x\to0$ and L.

Salmun *et al.* (1991) found from numerical computation a result comparable to (66), although their results indicated a variation in the coefficient in the range 1×10^{-6} to 3×10^{-5}. As our analysis shows, the coefficient varies weakly with β (figure 3) and in the vertical as determined by the density gradient. Furthermore, the analysis in §2 shows that this result is valid providing that the inertial terms in (29) or (41) are small in magnitude compared to the viscous terms.

As (66) shows, there is a very strong dependence of the effective interior diffusivity K_{I} on the boundary-layer thickness h. Typical interior diffusivities in lakes or reservoirs are of order 10^{-6} m^2 s^{-1}, while the buoyancy frequency can vary strongly over the seasonal stratification cycle or with depth (e.g. Imberger & Patterson 1990). Bottom diffusivities can vary between 10^{-4} m^2 s^{-1} and 10^{-6} m^2 s^{-1} and the slope θ can vary over the range 10^{-3} to 10^{-2}. In order to examine the effect of this variability in (66), we show in table 1 the values of h required to generate an effective interior

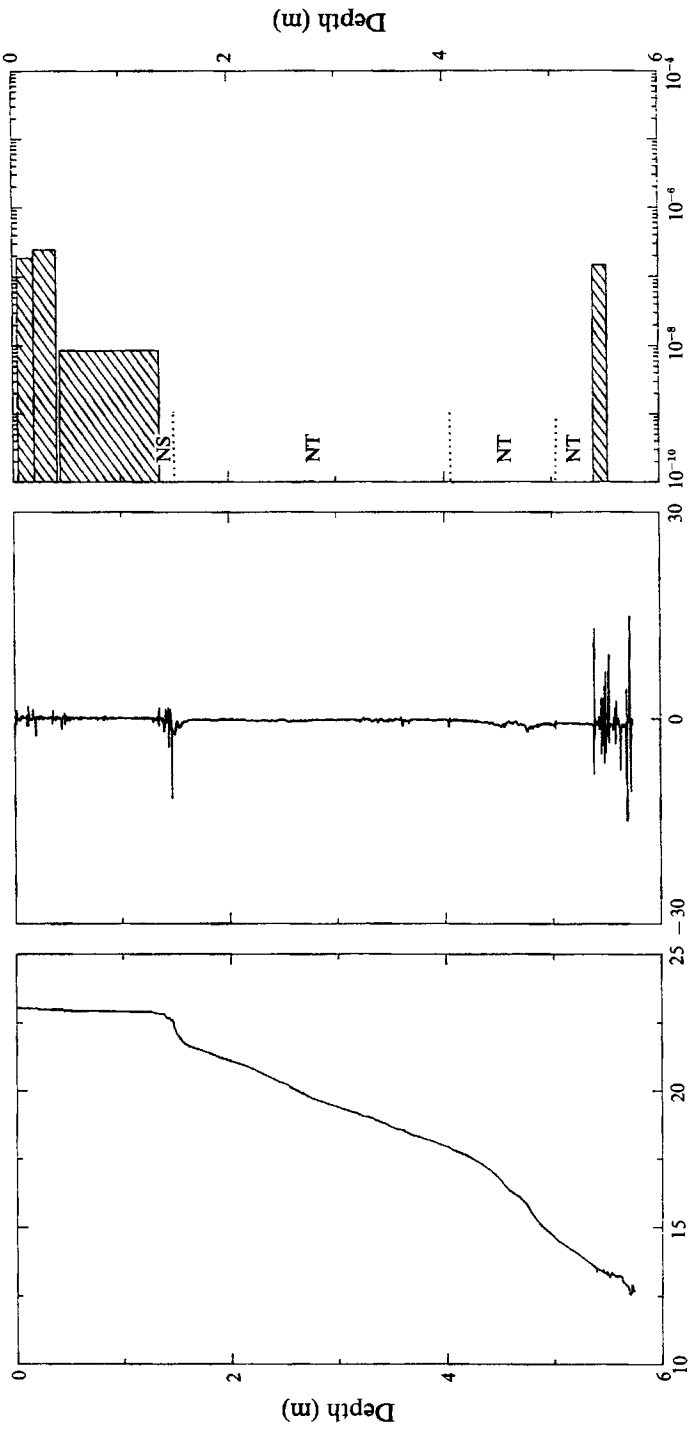

FIGURE 4. Temperature microstructure measurements in Lago di Lago (Venice). (NT means below noise threshold.)

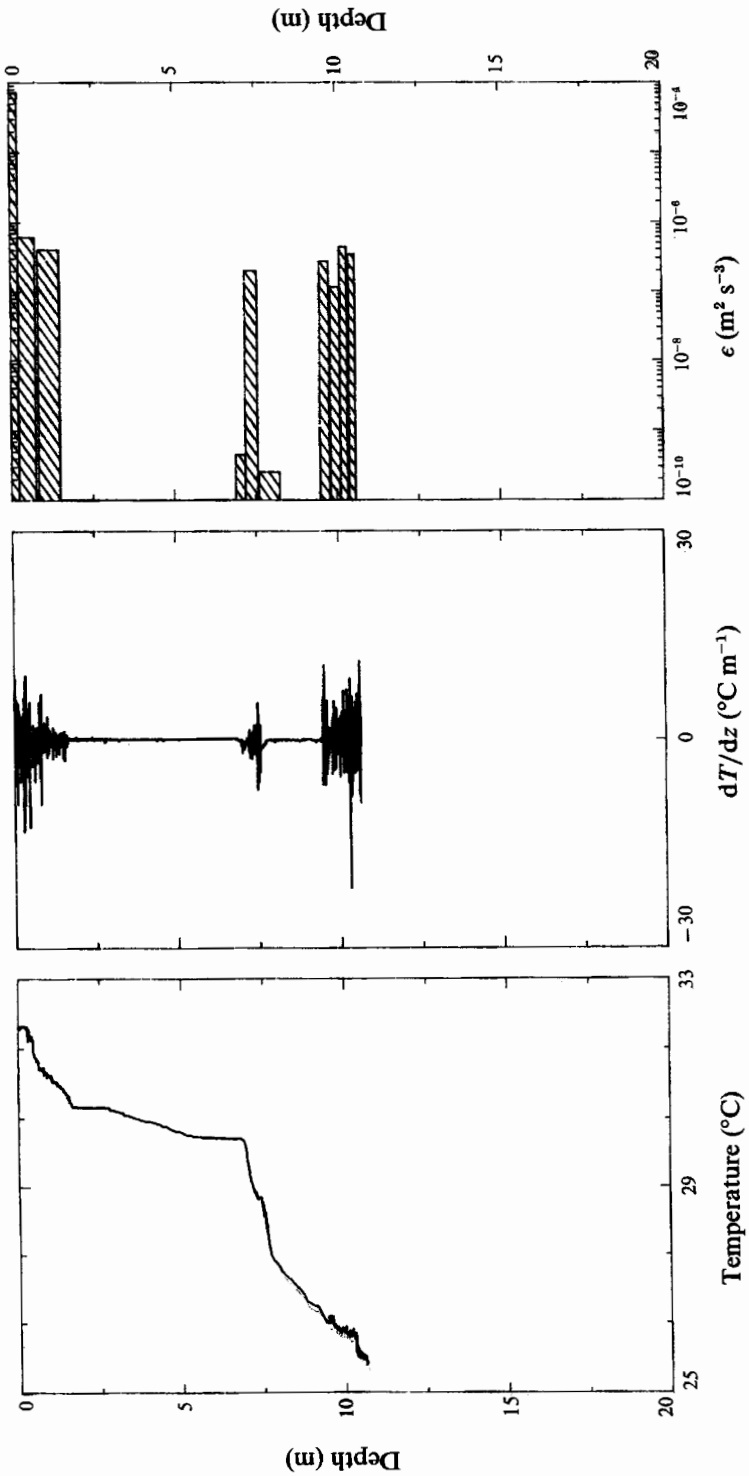

FIGURE 5. Temperature microstructure measurements in Lake Argyle.

diffusivity of $K_I = 10^{-6}$ m^2 s^{-1} in a basin with $l = 10^3$ m for a range of N, θ and ϵ. For extremely weak stratifications, the required h is 3–7 m. For the more realistic stratification likely to be found in the hypolimnion or thermocline, table 1 indicates that h varies between 0.2 and 2 m.

Table 1 also lists the parameter GrA^2 for each case, and for all cases $GrA^2 > 1$, implying at first inspection that inertial effects are indeed important. However, closer inspection of the velocity profile u_0' in (53) reveals that the average magnitude of u_0' over depth from 0 to 1 is $\bar{u} = 5.2 \times 10^{-3}(\mathrm{d}A/\mathrm{d}x)$ – a result confirmed by direct measurements of the velocity profile by Imberger (1974). Thus the best estimate of the ratio of the nonlinear to viscous terms over the boundary layer is

$$\frac{GrA^2(\partial/\partial z)(u'\,\partial u'/\partial x)}{\partial^3 u'/\partial z^3} \approx GrA^2(5 \times 10^{-3}),$$

implying $GrA^2 > 200$ before the inertial terms truly become important in the boundary-layer dynamics. This criterion is not satisfied for all realistic cases listed in table 1, and we conclude that the formulation in (66) can be applied.

In figures 4 and 5 we show examples of microstructure measurements of active mixing in the benthic boundary layer of two water bodies: Lago di Lago (Venice) in figure 4 and Lake Argyle (Western Australia) in figure 5. The two figures show temperature, temperature gradient and dissipation estimates (calculated using the techniques described in Imberger & Ivey 1991) over the water column where the bottom is 0.5 m beyond the bottom of the traces shown. In Lago di Lago, benthic mixing was forced by breaking internal waves with a boundary-layer thickness h of about 1 m, the rate of dissipation of turbulent kinetic energy $\epsilon_v = 10^{-7}$ m^2 s^{-3} and hence bottom diffusivities (from Fischer *et al.* 1979) are $\epsilon = 0.06\epsilon_v^{\frac{1}{3}} h^{\frac{4}{3}} = 3 \times 10^{-4}$ m^2 s^{-1}. The data in figure 5 are one sample from an extensive field experiment in Lake Argyle. Benthic mixing was forced by wind-driven bottom currents and the example in figure 5 has a background stratification of $N = 0.03$ rad s^{-1}, $\theta = 10^{-2}$, a layer thickness $h = 1.5$ m, dissipation $\epsilon_v = 4 \times 10^{-7}$ m^2 s^{-3}, and hence bottom diffusivity $\epsilon = 7 \times 10^{-4}$ m^2 s^{-1}. As table 1 indicates, such a parameter range is easily able to generate an effective interior diffusivity $K_I = 10^{-6}$ m^2 s^{-1} and the boundary mixing is thus significant in the deep mixing in the lake.

4. Conclusions

A perturbation analysis in the small parameter A, the aspect ratio of the turbulent boundary layer on the slope, shows that the primary force balance in the benthic boundary layer is a balance between viscous and buoyancy forces. For an arbitrary interior density profile, the solution predicts that a barotropic flow is established which is divergent along the slope, leading to a slow exchange between the boundary layer and the interior. The circulation thereby established in the interior can lead to changes in the interior density gradient which are significant when compared to field observations.

The authors thank S. G. Schladow, K. Zic, H. Salmun and our referees for comments on the manuscript.

REFERENCES

ARMI, L. 1978 Some evidence for boundary mixing in the deep ocean. *J. Geophys. Res.* **83**, 1971–1977.

BEJAN, A. & IMBERGER, J. 1979 Heat transfer by forced and free convection in a horizontal channel with differentially heated ends. *Trans. ASME* C: *J. Heat Transfer* **101**, 417–421.

CORMACK, D. E., LEAL, L. G. & IMBERGER, J. 1974 Natural convection in a shallow cavity with differentially heated end walls. Part 1. Asymptotic Theory. *J. Fluid Mech.* **65**, 209–229.

ERIKSEN, C. C. 1985 Implications of ocean bottom reflection for internal wave spectra and mixing. *J. Phys. Oceanogr.* **15**, 1145–1156.

FISCHER, H. B., LIST, E. J., KOH, R. C. Y., IMBERGER, J. & BROOKS, N. H. 1979 *Mixing in Inland and Coastal Waters*. Academic.

GARRETT, C. 1990 The role of secondary circulation in boundary mixing. *J. Geophys. Res.* **95**, 3181–3188.

GARRETT, C. 1991 Marginal mixing theories. *Atmos. Ocean* **29**, 313–339.

GILBERT, D. & GARRETT, C. 1989 Implications for ocean mixing of internal wave scattering off irregular topography. *J. Phys. Oceanogr.* **19**, 1716–1729.

GREGG, M. C. & SANFORD, T. B. 1980 Signatures of mixing from the Bermuda slope, the Sargasso Sea and the Gulf Stream. *J. Phys. Oceanogr.* **10**, 105–127.

IMBERGER, J. 1974 Natural convection in a shallow cavity with differentially heated end walls. Part 3. Experimental results. *J. Fluid Mech.* **65**, 247–260.

IMBERGER, J. 1989 Vertical heat flux in the hypolimnion of a lake. In *Proc. 10th AFMC, Melbourne, 1989*, vol. I, pp. 2.13–2.16.

IMBERGER, J. & IVEY, G. N. 1991 On the nature of turbulence in a stratified fluid, Part 2: Application to lakes. *J. Phys. Oceanogr.* **21**, 659–680.

IMBERGER, J. & PATTERSON, J. C. 1990 Physical limnology. *Adv. Appl. Mech.* **27**, 303–475.

IVEY, G. N. 1987 Boundary mixing in a rotating, stratified fluid. *J. Fluid Mech.* **183**, 25–44.

IVEY, G. N. & CORCOS, G. M. 1982 Boundary mixing in a stratified fluid. *J. Fluid Mech.* **121**, 1–26.

IVEY, G. N. & NOKES, R. I. 1989 Vertical mixing due to the breaking of critical internal waves on sloping boundaries. *J. Fluid Mech.* **204**, 479–500.

LEDWELL, J. R. & WATSON, A. J. 1991 The Santa Monica Basin tracer experiment: A study of diapycnal and isopycnal mixing. *J. Geophys. Res.* **96**, 8695–8718.

MACCREADY, P. & RHINES, P. B. 1991 Buoyant inhibition of Ekman transport on a slope and its effect on stratified spin-up. *J. Fluid Mech.* **223**, 631–661.

MUNK, W. H. 1966 Abyssal Recipes. *Deep-Sea Res.* **13**, 707–730.

PHILLIPS, O. M. 1970 On flows induced by diffusion in a stably, stratified fluid. *Deep-Sea Res.* **17**, 435–443.

PHILLIPS, O. M., SHYU, J.-H. & SALMUN, H. 1986 An experiment on boundary mixing: mean circulation and transport rates. *J. Fluid Mech.* **173**, 473–499.

SALMUN, H., KILLWORTH, P. D. & BLUNDELL, J. R. 1991 A two-dimensional model of boundary mixing. *J. Geophys. Res.* **96**, 18,447–18,474.

SALMUN, H. & PHILLIPS, O. M. 1992 An experiment on boundary mixing. Part 2. The slope dependence at small angles. *J. Fluid Mech.* **240**, 355–377.

TAYLOR, G. I. 1954 Observations of the atmospheric boundary layer over the ocean. *Proc. R. Soc. Lond.* A **223**, 446–468.

THORPE, S. A. 1982 On the layers produced by rapidly oscillating a vertical grid in a uniform stratified fluid. *J. Fluid Mech.* **124**, 391–409.

THORPE, S. A. 1987 Current and temperature variability on the continental slope. *Phil. Trans. R. Soc. Lond.* A **323**, 471–517.

THORPE, S. A., HALL, P. & WHITE, M. 1990 The variability of mixing at the continental slope. *Phil. Trans. R. Soc. Lond.* A **331**, 183–194.

WOODS, A. W. 1991 Boundary-driven mixing. *J. Fluid Mech.* **226**, 625–654.

WUNSCH, C. 1970 On oceanic boundary mixing. *Deep-Sea Res.* **17**, 293–301.

YOUNG, W. R. & JONES, S. 1991 Shear dispersion. *Phys. Fluids* A **3**, 1087–1101.